J Mater Sci (2009) 44:4031–4039
DOI 10.1007/s10853-009-3562-0

Decyl bis phosphonate–protein surface modification of Ti–6Al–4V via a layer-by-layer technique

Yu Xiang Ni · Bo Feng · Jianxin Wang · Xiong Lu · Shuxin Qu · Jie Weng

Received: 5 March 2009 / Accepted: 11 May 2009 / Published online: 26 May 2009
© Springer Science+Business Media, LLC 2009

Abstract Titanium and its alloys have been applied in orthopedics due to their biocompatibility, mechanical, and physical properties. Here we use decyl bis phosphonate (DBP) and collagen I to modify Ti–6Al–4V through layer-by-layer technique in order to improve its bioactivity. The abilities of bovine serum albumin (BSA) adsorption and biomimetic mineralization of different sample surfaces were studied. X-ray photoelectron spectroscopy (XPS) and water contact angle data showed that DBP and collagen I were assembled on substrates successfully. The absorbance of BSA solution acquired from ultraviolet spectrophotometer (UV) indicated that samples of Ti–6Al–4V/DBP/Collagen and Ti–6Al–4V/DBP/Collagen/DBP adsorbed BSA most, followed by Ti–6Al–4V/DBP and Ti–6Al–4V. Scanning electron microscope (SEM) photos and X-ray diffraction (XRD) data showed that sample of Ti–6Al–4V/DBP/Collagen had better bioactivity in inducing HA formation than other samples tested in this investigation.

Introduction

Titanium and its alloys (notably Ti–6Al–4V) have high mechanical strength and are resistant to chemical attack [1], thus they are of increasing importance in fields as diverse as aviation and aerospace, high-performance sports equipment, and medical implants. The orthopedic and dental implants industry is largely based on the favorable interfacial interaction at the bone–titanium interface [2, 3]. However, even though titanium has good biocompatibility, it can only be integrated with bone passively, and it cannot directly bind to bone [4]. As a result, the surface modification of titanium and its alloys is badly needed.

Layer-by-layer (LBL) self-assembly technique, which is based on the consecutive adsorption of polyanions and polycations via electrostatic interactions, and is considered as a versatile, inexpensive yet efficient technique to "build'' biologically active surfaces in recent years [5, 6]. Phosphate is argued to be one of the essential elements for life on earth, and some of its important properties include a stable oxidation state, a buffering capacity, and range near pH 7 [7]. Long-chain phosphonic acids or alkylphosphoric acids can chelate strongly with a wide range of alkali and transition metals. They can form highly oriented and well-ordered self-assembled monolayers (SAMs) without polymerization similar to thiols SAM on gold [8]. Therefore, alkyl-phosphonic acid and its corresponding phosphonate, including hexadecyl phosphoric acid ester [8], octylphosphonic acid [9], dodecyl phosphoric acid [10], octadecylphosphonic acid [2], and α-quarterthiophene-2-phosphonate [11] were used as SAMs bind directly to the native oxide metal surfaces. These studies showed the monolayers were bonded to the metal surface through phosphonic acid groups, and the surface components, surface loadings, as well as morphologies were investigated. However, the monolayers discussed above have only one active functional group (phosphonic acid group), and their tail group, methyl, was an inert group. As a result, these monolayers were difficult to be further activated. Danahy MP [12] assembled 1,12-diphosphonododecane on the surface of titanium. Both the head group and tail group were phosphonic acid group in 1,12-diphosphonododecane, and when the head group had linked with titanium surface,

Y. X. Ni · B. Feng (✉) · J. Wang · X. Lu · S. Qu · J. Weng
Key Laboratory of Advanced Technologies of Materials, Ministry of Education, School of Materials Science and Engineering, Southwest Jiaotong University, Chengdu 610031, People's Republic of China
e-mail: fengbo@swjtu.edu.cn

the tail group were further reacted with zirconium tetra and peptide. The modified surfaces were shown to be effective for osteoblast binding and proliferation. Similarly, 11-hydroxyundecylphosphonic acid [13] was assembled on Ti–6Al–4V, and DANSYL–cysteine was bonded to Ti–6Al–4V via an 11-hydroxyundecylphosphonate interface. The hydrolytic stability of the phosphonate interface was tested to be robust.

Different tail groups can be introduced to the substrate via SAM technique, and biological molecules can then be immobilized on the SAM modified surface [14]. In this study, we used decyl bis phosphonate (DBP, $C_{10}H_{24}P_2O_8$) and collagen I to assemble on the surface of Ti–6Al–4V alternately via a LBL self-assembly technique. DBP, one of alkyl bis-phosphates, is a kind of strong acid [15], and both its head group and tail group are phosphonic acid group. Its hydrions in acidic hydroxyls are likely to dissociate when dissolved in solvent, leaving the rest molecule electronegative [16]. Collagen I is a protein that takes up 95% of the organic components in bone tissues [17], and it is widely used in the food, pharmaceutical, cosmetic, biomedical materials, and leather industries [18]. As a kind of protein, collagen I is an ampholyte, and its isoelectric point (PI) is 8.3 [19]. When the solvent pH is less than PI, it will be positively charged. Therefore, DBP and collagen I can be combined together through electrostatic attractions. With its excellent biological activity, we expect the existence of collagen I can play a positive role in improving the biocompatibility of Ti–6Al–4V.

Biomineralization and protein adsorption tests are important means for evaluating implants' stabilization [20, 21]. The initial stage involved in the adhesion of cells and the formation of biofilms on solid surfaces is the adsorption of proteins present in the medium. In particular, the interaction between cells and the surface of biomedical implants is mediated by pre-adsorbed proteins [22]. It has been indicated that initial protein adsorption is important for the integration of a titanium bone implant [23]. Bovine serum albumin (BSA) was chosen as the model protein as it is available in a highly purified form, easily soluble in water and homogeneous [24]. And it is also commonly used as a model protein for studying protein–surface interactions [22].

The previous study has proved alkyl-phosphates or alkyl-diphosphonic acids could be self-assembled successfully on titanium and its alloys [2, 8–13], however, the biocompatibilities of these modified surfaces such as protein adsorption and biomimetic mineralization have not been discussed yet. To our best knowledge, this is the first time that alkyl-bis phosphate and collagen I were formed on Ti–6Al–4V via a LBL technique, and the focus of our study is on the investigation of the protein adsorption and biomimetic mineralization of these modified surfaces.

Materials and methods

General

The Ti–6Al–4V specimens used in the experiments were commercial Ti–6Al–4V (Baoji Special Iron and Steel Co. Ltd., China) with dimensions of 10 mm × 10 mm × 1 mm. The disks were sanded first with 600, 1000, 1500, and 2000 grit silicon carbide paper, rinsed with sonication successively with acetone, ethanol, hot methanol, and deionized H_2O, dried, and stored in an oven at 160 °C for 2 h, which gives a surface coating of hydroxylated titanium dioxide [2]. 1,10-Decanodiol (97%, Aldrich) and rat collagen I (100 mg/20 mL, Trevigen. Inc.) were used as received. Tetrahydrofuran (THF) was distilled over Na and stored under argon. Phosphorus oxychloride was also distilled and stored under argon. All reagents were analytical grade or better, and purchased from Changzheng Regents Company (China), unless otherwise indicated. Synthesized decyl bis phosphonate (DBP) was characterized by ^{1}H NMR (VarianUnity, IVOVA—400 MHz). Fourier transform infrared spectroscopy (FTIR, Nicolet 5700, Thermo, USA) was used to determine the functional group of DBP and adsorbed BSA on sample surfaces, and the spectra were collected over the range of 4000–500 cm^{-1}. Chemical compositions of the self-assembled surfaces were determined by X-ray photoelectron spectroscopy (XPS, XSAM800, Kratos Ltd, Britain) using Mg $K\alpha$ 1,2 radiation, and data were processed using Kratos VISION 2000. The overview spectra were taken between 50 and 1300 eV with an energy step of 0.5 eV using pass energy of 300 eV, while the detailed spectra of peaks of interest (Ols, Cls, P2p, and N1s) were recorded with an energy step of 0.05 eV. The water contact angle of the samples were measured on a Kruss GmbH DSA 100Mk 2 goniometer (Germany) followed by image processing of sessile drop with DSA 1.8 software. At least five droplets were tested on different parts of each sample surface. The absorbance of bovine serum albumin (BSA) solution was determined at 278 nm wavelength with an ultraviolet spectrophotometer (UV, UV-2550, Japan), and fluorescence microscope (Leica DMR, Germany) was used to collect the surface protein images. The phases of the substrates and the coatings were identified using a thin film X-ray diffractometer (TF-XRD, X'pert pro-MPD, PANalytical, The Netherlands). The TF-XRD measurements were performed on a stage using a Cu-$K\alpha$ (wavelength = 1.54056 Å) X-ray source from 20° to 50° with a step rate of 0.01° per second. The morphology of surface coatings was observed with scanning electron microscope (SEM, FEI Quanta 200, The Netherlands) operated at an accelerating voltage of 20 kV.

Synthesis of decyl bis phosphonate (DBP)

Phosphorus oxychloride (2.50 g, 16.32 mmol) was added in a three-necked bottle (250 mL) previously. 1,10-Decanodiol (1.42 g, 8.16 mmol) was dissolved in 50 mL of dry, distilled THF, and then added in a dropping funnel (250 mL). The solution was dropped slowly into the three-necked bottle under dry N_2, and the reaction mixture was allowed to stir at 5–10 °C for 8 h. After that, deionized H_2O (D-H_2O) (1.0 g, 55.55 mmol) was added to the reaction mixture and stirred at 40–50 °C for 2 h [16]. The solvent was then removed to give yellow, oily crude DBP, which was then treated by sodium hydroxide to form mono sodium salt of alkyl phosphate. The mono sodium salt was purified by recrystallization from methanol, and acidified to restore to DBP [25]. Purified DBP was characterized by FTIR (νCH_2(asymm) = 2930 cm^{-1}, νCH_2(symm) = 2850 cm^{-1}, νP–OH = 2340 cm^{-1}, νP–O–C = 1020 and 837 cm^{-1}) and ^{1}H NMR (acetone-d6): δ(ppm) 1.34-1.39 (m, P–O–$CH_2CH_2(C\mathbf{H}_2)_6CH_2CH_2$–O–P, 12H), 1.64–1.69 (m, –$CH_2C\mathbf{H}_2(CH_2)_6C\mathbf{H}_2CH_2$–, 4H), 3.96–4.00 (m, –$C\mathbf{H}_2CH_2(CH_2)_6CH_2C\mathbf{H}_2$–, 4H).

Preparation of DBP and collagen I films on Ti–6Al–4V

Polished disks of Ti–6Al–4V were suspended vertically in dilute solutions of DBP (0.05 mM/L in dry THF) in a beaker. The solvent was allowed to evaporate so that the meniscus slowly traversed the disk surface to give the SAM of DBP, and the evaporation time was about 2 days. Coated disks were then heated in an oven at 140 °C for 48 h to convert this film to the SAM of the phosphonate [12]. The disks were then rinsed extensively in methanol and D-H_2O and dried in air. The disks treated above were marked as Ti–6Al–4V/DBP (T/P for short). Collagen I was dissolved in phosphate buffer solution (PBS) at room temperature with the concentration of 25 μg/mL. The PBS was prepared by dissolving chemicals of NaCl, KCl, KH_2PO_4, and Na_2HPO_4 into D-H_2O and buffered at pH 6.80 with 0.1 mol/L HCl or NaOH. This pH belows the isoelectric point (PI) of collagen I (8.3), thus collagen I can be positively charged when dissolved in PBS. T/P disks were then immersed in collagen I/PBS solution under room temperature for 4 h, then washed extensively with PBS, dried in vacuum drying oven (25 °C, 1.325 × 10^{-3} MPa) for 20 min and stored at 4 °C. These disks were marked as Ti–6Al–4V/DBP/collagenI (T/P/C for short). After that, T/P/C disks were treated in DBP/THF solution again following the procedures mentioned above (without heating), then washed extensively with PBS, dried in vacuum drying oven (25 °C, 1.325 × 10^{-3} MPa) for 20 min and stored at 4 °C to give disks of Ti–6Al–4V/DBP/collagenI/DBP (T/P/C/P for short). The Chemical compositions of the three surfaces (T/P, T/P/C and T/P/C/P) were detected by XPS, and the water contact angles of the samples were also measured.

BSA adsorption

Samples of T/P, T/P/C, T/P/C/P as well as Ti–6Al–4V were immerged in 45 mL BSA/PBS solution (1 mg/mL, pH = 7.3) at 37 °C. One milliliter of BSA solution was taken out after 0.5, 1, 2, 4, 8, 12, and 24 h, respectively. According to Lambert–Beer law, the absorbance of a solution is directly proportional to its concentration at a given wavelength of light. The absorbance of BSA solution at different time points was measured at 278 nm wavelength by UV. The concentration was obtained using a standard curve from known concentrations of BSA solutions, and the curves of adsorption quantity-time were plotted. *T*-tests were performed to determine any differences between adsorbed protein quantities of different samples. Data are reported at a significance level of $p < 0.05$.

The samples were then taken out from BSA solution, tested by IR, and then treated by glutaraldehyde solution (1%, 5 min) and fluorescein/ethanol solution (5 mg/mL, 10 min), washed extensively by PBS, and observed by fluorescence microscopy.

Biomimetic mineralization

Simulated body fluid (SBF), which is compositionally similar to human body fluid, has been frequently used to apply biomimetic apatite coatings on various biomaterials [26]. In order to accelerate the deposition of apatite on the surface, we used two SBF in this experiment. Two SBF has ionic concentrations two times of that of normal SBF. The composition of two SBF is as follows (in mmol): Na^+ 284.0, K^+ 10.0, Mg^{2+} 3.0, Ca^{2+} 5.0, Cl^- 295.6, HCO^{3-} 8.4, HPO_4^{2-} 2.0, and SO_4^{2-} 1.0. The solution was prepared by dissolving NaCl, $NaHCO_3$, KCl, K_2HPO_4, $MgCl_2 \cdot 6H_2O$, $CaCl_2$ and Na_2SO_4 into D-H_2O and buffered at pH 7.4 (37 °C) with tris–hydroxymethyl aminomethane, and 0.1 mol/L HCl. Each sample was immersed in 20 ml 2 SBF in a plastic tube. The tubes were placed in a shaking water bath at 37 °C. The solution was refreshed every 24 h. Seven days later, the samples were taken out, washed with D-H_2O, dried in air, and measured by XRD and SEM.

Results

Preparation of DBP and collagen I films on Ti–6Al–4V

XPS was used to monitor surfaces of T/P, T/P/C and T/P/C/P as it can provide information on chemical structure and surface contamination. Figure 1 shows the overview

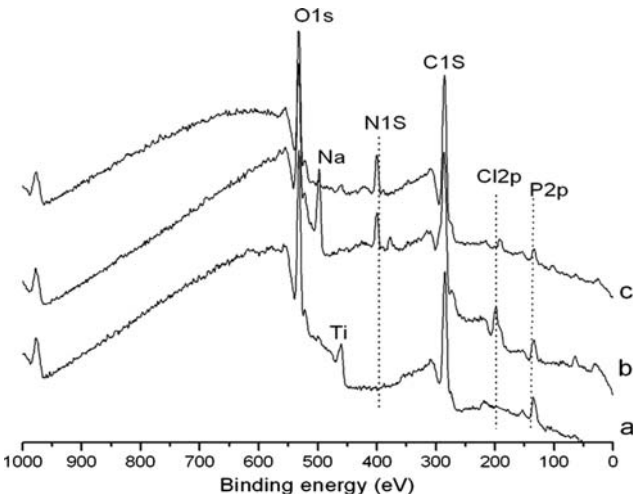

Fig. 1 Results of XPS surface analysis: overview spectra of: (a) T/P; (b) T/P/C; (c) T/P/C/P

spectra of the three surfaces. O1s, C1s, and P2p spectra were detected on all the three samples, indicating the existence of DBP on the three surfaces. N1s spectra was detected on both T/P/C and T/P/C/P surfaces, but not on T/P, which provides the evidence that collagen I was assembled on the samples of T/P/C and T/P/C/P successfully. Meanwhile, peaks of Cl and Na on T/P/C and T/P/C/P shows that NaCl from PBS was probably existed on these two surfaces.

Figure 2 shows the evolution of the XPS signals of O1s, C1s, and P2p from T/P, T/P/C and T/P/C/P, and N1s from T/P/C and T/P/C/P. Table 1 lists the experimental XPS binding energies of the deconvoluted detailed spectra and the proposed assignments to chemical bonds/oxidation states based on chemical shifts.

The values of the water contact angle (°) and surface energy (mN/m) of the treated samples as well as Ti–6Al–4V are presented in Fig. 3. Surface energy was calculated by the formula of equation of state (EOS). We observed a significant increase of contact angles of T/P and T/P/C/P from 35.5 ± 2° (Ti–6Al–4V) to 53.0 ± 2° and 72.3 ± 3°, respectively. This increase was probably due to the presence of CH_2, which is a hydrophobic group that takes up a large proportion of DBP. However, in contrast with T/P and T/P/C/P, the contact angle of T/P/C was 11.2 ± 1°, which was lower than that of Ti–6Al–4V. This is because collagen I is a hydrophilic material and the C–OH bonding in it can form a strong hydrogen bond with the water molecules [27].

BSA adsorption

The FTIR spectra of adsorbed BSA on different surfaces are shown in Fig. 4. The signal at 1650 cm^{-1} is assigned to C=O stretching and amide N–H bending for the amide I. The signal at 1545 cm^{-1} is N–H deformation for the amide

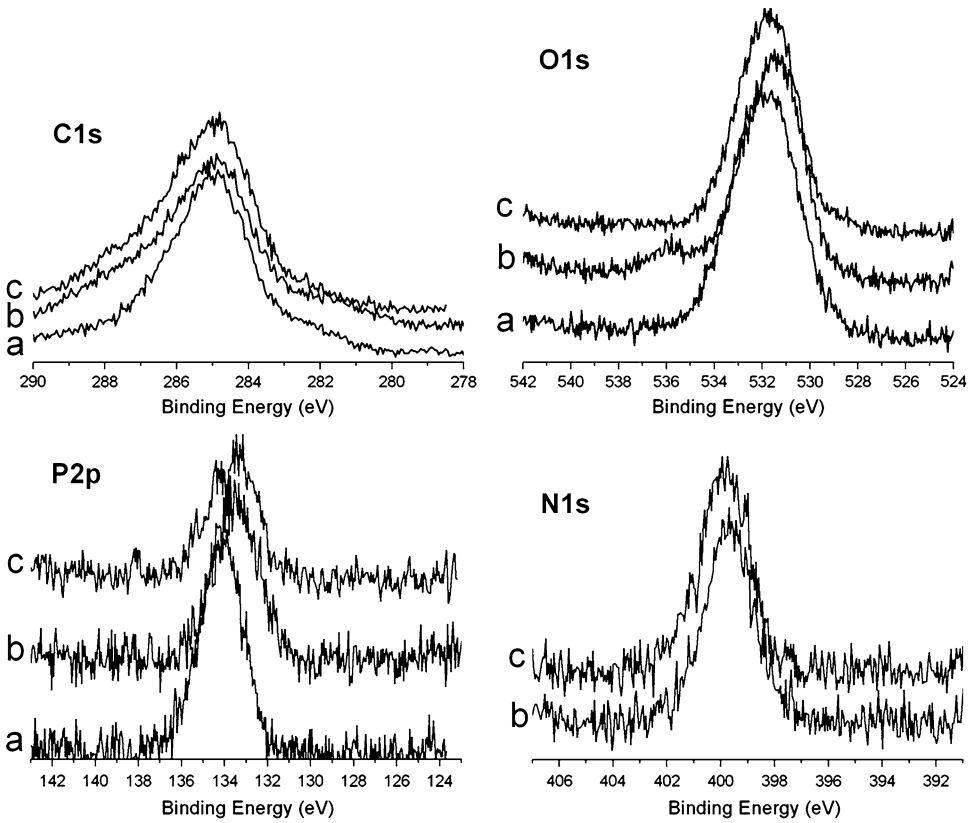

Fig. 2 Results of the XPS surface analysis: evolution of C1s, P2p, O1s, and N1s spectra from T/P, T/P/C, and T/P/C/P

Table 1 XPS binding energies of C1s, O1s, P2p, and N1s for the surfaces of T/P, T/P/C and T/P/C/P and the proposed assignments to surface functionalities

Surface	C1s region BE (eV), %, assignments	O1s region BE (eV), %, assignments	P2p region BE (eV), %, assignments	N1s region BE (eV), %, assignments
T/P	284.90(71) C–H	530.90(2) TiO_2	134.13(100) P–OH	
	285.73(19) C–C	532.27(98) phosphate		
	286.80(10) C–O–P			
T/P/C	284.78(65) C–H	530.84(9) TiO_2	133.50(100) $P–O^-$	399.22(52) NH_2
	285.62(18) C–C	531.24(67) phosphate		400.22(48) NH_3^+
	287.08(13) amide–C	532.30(24) COOH		
	288.31(4) imide–C			
T/P/C/P	284.81(65) C–H	530.10(2) TiO_2	133.38(67) $P–O^-$	399.22(32) NH_2
	286.03(21) C–C	531.53(79) phosphate	134.09(33) P–OH	400.22(68) NH_3^+
	286.99(10) amide–C	532.86(19) COOH		
	288.25(4) imide–C			

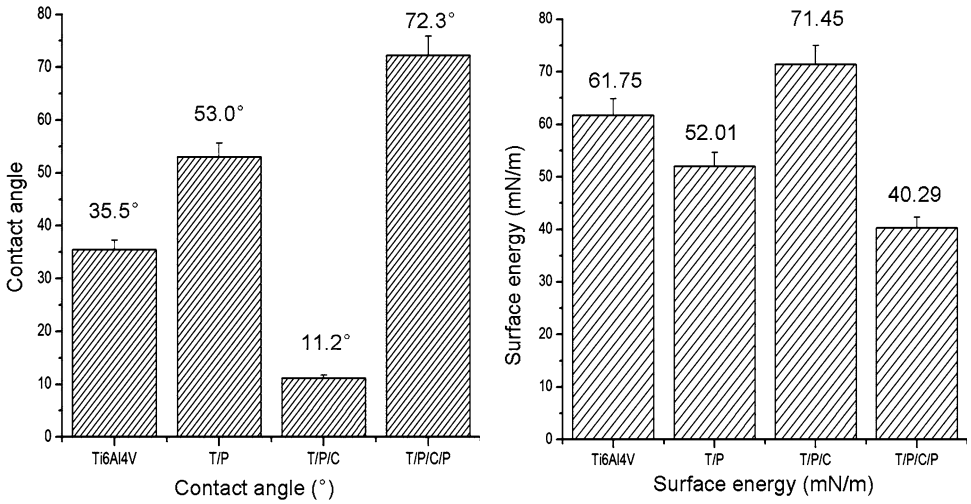

Fig. 3 Water contact angle and surface energy of Ti–6Al–4V, T/P, T/P/C, and T/P/C/P

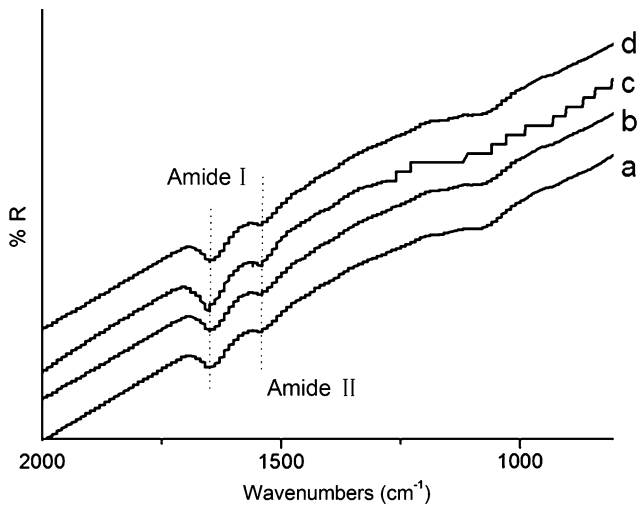

Fig. 4 FTIR spectra of BSA adsorption for 24 h on samples with (a) Ti–6Al–4V; (b) T/P; (c) T/P/C; (d) T/P/C/P

II of BSA secondary structure [28]. FTIR spectra suggested BSA was adsorbed on all the samples.

Figure 5 shows the fluorescence microscopy photographs of samples adsorbed BSA. As the intensity of fluorescence is in direct proportion to the amount of BSA adsorbed on the sample surfaces, we can acquire the relative amount and distribution information of the surface BSA. As is shown in Fig. 5, the intensity of fluorescence of T/P/C and T/P/C/P were the highest, followed by T/P and Ti–6Al–4V.

Figure 6 displays the adsorption quantity of BSA at different time points of the four samples. Within 0.5 h, BSA rapidly adsorbed onto all surfaces. Twelve hours later, the quantity of adsorbed BSA gradually reached the equilibrium on every sample. Finally, the BSA adsorption on Ti–6Al–4V, T/P, T/P/C and T/P/C/P are 19.50 mg, 20.83 mg, 26.10 mg, and 24.33 mg, respectively. These data indicate samples of T/P, T/P/C, and T/P/C/P adsorbed

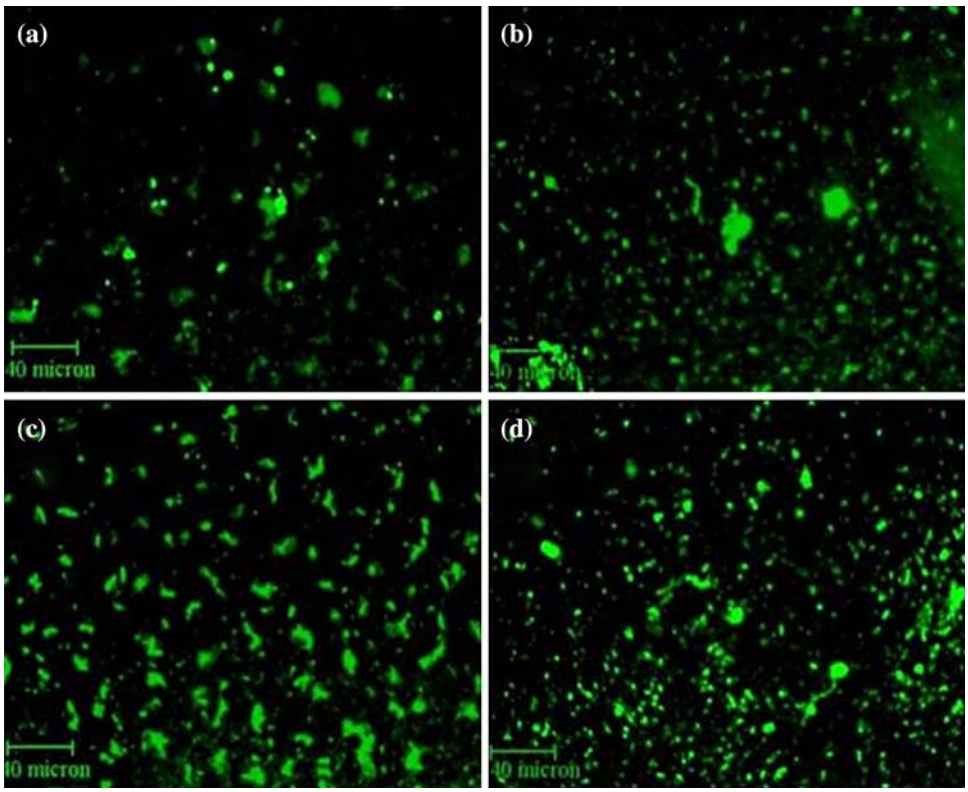

Fig. 5 Fluorescence microscope photographs of BSA adsorbed samples: (**a**) Ti–6Al–4V; (**b**) T/P; (**c**) T/P/C; (**d**) T/P/C/P

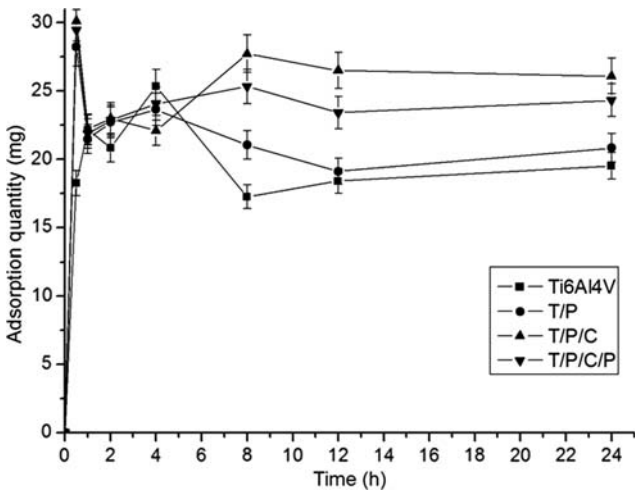

Fig. 6 The curves of adsorbed BSA quantity-time on samples with (*filled square*) Ti–6Al–4V; (*filled circle*) T/P; (*filled triangle*) T/P/C; (*reverse triangle*) T/P/C/P

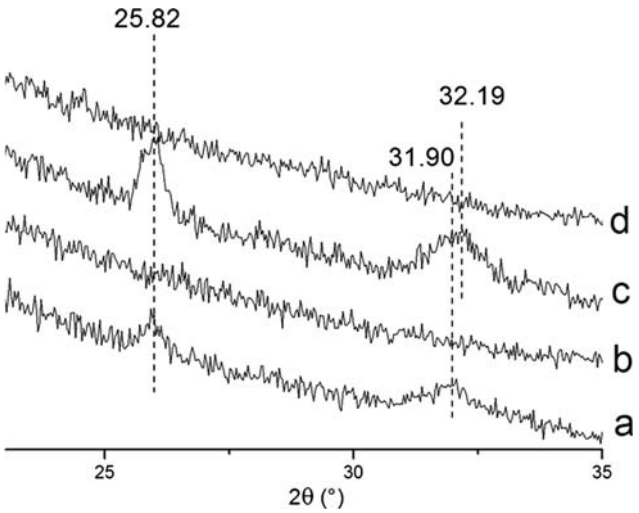

Fig. 7 XRD patterns of samples after Biomimetic mineralization treatment: (a) Ti–6Al–4V; (b) T/P; (c) T/P/C; (d) T/P/C/P

more BSA than Ti–6Al–4V ($p < 0.05$). This result is consistent with Fig. 5.

Biomimetic mineralization

Figure 7 shows the XRD patterns of four sample surfaces after soaked in Two SBF for 7 days. No apatite peak could be found in XRD patterns of T/P and T/P/C/P, whereas hydroxyapatite (HA) peaks could be seen for Ti–6Al–4V and T/P/C (JCPDS file number: 01-074-0566). Peaks of 25.89, 31.90, and 32.19 correspond to (002) plane, (211) plane and (112) plane of HA, respectively.

The SEM images indicate consistent results with XRD (Fig. 8). No uniform coating formed on the surfaces of T/P and T/P/C/P and its original morphology could be clearly seen (Fig. 8b, d). A lot of apatite coatings could be seen on the surfaces of Ti–6Al–4V (Fig. 8a), while in Fig. 8c, T/P/C was obviously covered with apatite coating. This result

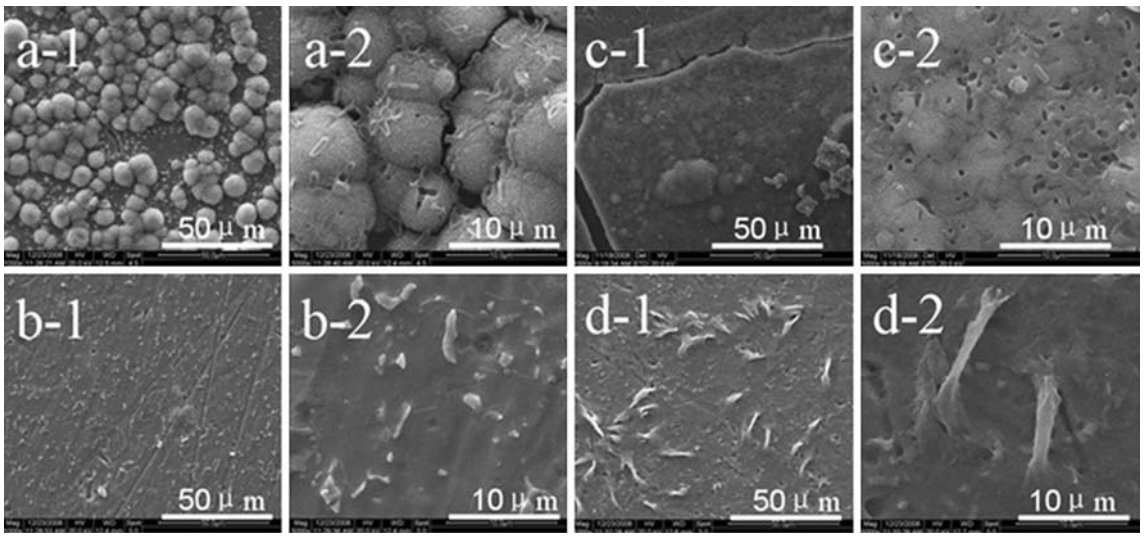

Fig. 8 SEM images of samples soaked in two SBF for 7 days with (**a**) Ti–6Al–4V; (**b**) T/P; (**c**) T/P/C; (**d**) T/P/C/P

revealed that the T/P/C surface has good ability for biomineralization but the DBP terminated surfaces were not favorable to the apatite growth.

Discussion

The presence of P2p and N1s spectra in Fig. 1 showed that DBP and collagen I were assembled on Ti–6Al–4V successfully. The change of chemical environment is an important factor that causes the displacement of spectra peak [29]. Judging from Fig. 2 and Table 1, the binding energy of P2p from T/P/C (133.50 eV) was lower than that from T/P (134.13 eV), indicating the electronegativity of phosphor in T/P/C was stronger than that of T/P. In other words, when immersed in collagen I/PBS solution, the hydrions in acidic hydroxyls of DBP in T/P were probably dissociated, thus DBP was negatively charged and reacted with collagen I to form T/P/C. According to Table 1, the percentage of NH_3^+ increased from 48% (in T/P/C) to 68% (in T/P/C/P), that means compared to T/P/C, more amino-groups in T/P/C/P had transformed to NH_3^+ and reacted with DBP. These data provide the evidence that DBP and collagen I were combined together through electrostatic attractions between $P–O^-$ and NH_3^+ rather than physical adsorption. No peak for $Ti2p_{3/2}$ was detected in T/P/C and T/P/C/P, indicating a thick and fully covered collagen I film was prepared on the two surfaces. Meanwhile, the presence of Cl and Na on T/P/C and T/P/C/P shows NaCl from PBS was probably existed on these two surfaces and it was difficult to get rid of it because the samples of T/P/C and T/P/C/P were washed by PBS. However, it will not cause any negative effect to the biocompatibility of the samples since NaCl is widely existed in human body.

Samples of T/P were rinsed extensively in methanol and D-H_2O, while in order to protect protein in samples of T/P/C/P, they were only washed with PBS. Methanol is a good solvent for DBP but PBS is not. In that case, physically adsorbed DBP on T/P/C/P may not be easily washed out by PBS, which in turn left more DBP on T/P/C/P than T/P. This might be the reason why the water contact angle significantly increased from 53.0 ± 2° (T/P) to 72.3 ± 3° (T/P/C/P) while in both cases the top surface layer was the same (DBP). More studies should be done to investigate how much amount of DBP and collagen I were loaded on Ti–6Al–4V.

The ability of biomaterials to absorb protein relies heavily on its surface functional group, surface charge, surface energy, and surface morphology [30]. Figures 5 and 6 manifest that the samples of T/P/C and T/P/C/P adsorbed BSA most, followed by T/P and Ti–6Al–4V. On one hand, it can be attributed to the surface functional groups in T/P/C, such as $–NH_2$ and –COOH. These functional groups may react with BSA actively, probably through peptide bond and hydrogen bond. The existence of phosphate radical in T/P, T/P/C, and T/P/C/P may also play an important role in protein absorption. On the other hand, the charge of both protein and the surface is another important factor in determining the amount of protein adsorbed on surfaces [31]. The pH of PBS we used for BSA adsorption was 7.3, which was above the isoelectric point of BSA (4.7), and was below the isoelectric point of collagen I (8.3). Thus, BSA was negatively charged and collagen I was positively charged over the working pH range. Therefore, electrostatic effects were important in the interaction of the BSA with the T/P/C and T/P/C/P surfaces.

It is reported that surface energy also has significant influences in protein absorption of biomaterials, and the

hydrophobic surfaces are more likely to absorb protein than hydrophilic surfaces [30, 32]. It seems to be inconsistent to our experimental data where the more hydrophilic surface sample, T/P/C, adsorbed BSA more. Actually, this conclusion is not a universal rule and it depends on the protein and the specific surface. Generally, the protein adsorption on hydrophilic surfaces can be associated with water structure at the surface, electrostatic interactions and the conformational changes of the protein [33]. For sample of T/P/C in this study, the interaction of functional groups between substrate and BSA and their electrostatic effects, which were mentioned above, might be the driving force in protein adsorption. For samples of T/P and T/P/C/P, both of whose surface energy were above 20 mN/m, the protein adsorption mechanism can be explained as follows: to the surfaces with adhesion tension above 20 mN/m, the interfacial energy increases because of protein adsorption. In order to compensate this energetically unfavorable increase, protein was probably expelled from the bulk of the water which can be seen as hydrophobic attraction between the protein and the substrate [34].

The wettability of material surfaces generally depends on two major factors: chemical functionality and/or surface roughness [35]. Changes in either surface chemistry or morphology will contribute to the observed value of the contact angle [27]. In this study, both the surface chemistry and surface morphology might be changed, which resulted in contact angle changes. However, here we have only investigated the surface chemical changes of the samples. More work should be done to further study how the surface roughness affected the value of the contact angle and surface energy.

HA, whose chemical formula is $Ca_{10}(PO_4)_6(OH)_2$, is quite similar to the materials forming the bones in the human body [36]. Also, HA is thought to be a particularly attractive coating material as it has been shown to induce chemical bonding at HA–bone interfaces and promote bone growth with high growing in rates [37]. Judging from our investigation, the sample of T/P/C showed best ability to induce HA formation. This was probably because T/P/C sample had protein terminated surface, which was full of functional groups such as $–NH_2$ and –COOH. The pH of SBF used here was 7.4, which was below the isoelectric point of collagen I. In that case, the collagen I on the sample was positively charged when it was immersed in SBF [38], which means NH^{3+} groups were presented on the surface of T/P/C. In accordance with Luong LH's study [39], the NH^{3+} groups of collagen I would bind to the PO_4^{3-} groups in SBF, and induce the formation of apatite. This is probably because the surface functional groups, which are capable of binding soluble ionic precursors, may become sites for the surface nucleation [40]. On the contrary, the DBP terminated surfaces (T/P and T/P/C/P) were not inductive to the HA growth. Although it is reported that the phosphate radical is favorable in HA formation, however, the abundant existence of methylene in DBP was to the disadvantage of the formation of HA because the ion-induced dipole interaction between the hydrocarbon and Ca^{2+} ion was too weak to participate in apatite nucleation [26, 40]. This may explain why the HA formation on T/P and T/P/C/P was poor.

Our future study focuses on the studies of the amount of DBP and collagen I loaded on Ti–6Al–4V surface and the stability of DBP and collagen I films on substrates under physiological environment using Quartz Crystal Microbalance (QCM), and the interactions of human osteoblasts with modified surfaces.

Conclusions

DBP and collagen I films were self-assembled on Ti–6Al–4V successfully through electrostatic interactions. The samples with collagen (T/P/C and T/P/C/P) showed the best ability in absorbing BSA, followed by T/P and Ti–6Al–4V. T/P/C also exhibited its good bioactivity in inducing HA formation whereas no HA layer was formed on DBP terminated surfaces (T/P and T/P/C/P). It is suggested that layer by layer technique using DBP and collagen I might be an effective way to improve the biocompability of Ti–6Al–4V.

Acknowledgements This study was jointly supported by the Chinese NSFC (50871093), FANEDD (200554), and National Key Project of Scientific and Technical Supporting Programs funded by MSTC (2006BAI16B01). The authors gratefully acknowledge Dr. Yuancong Zhao for kindly providing guidance in DBP synthesis.

References

1. Gawalt ES, Avaltroni MJ, Danahy MP, Silverman BM, Hanson EL, Midwood KS, Schwarzbauer JE, Schwartz J (2003) Langmuir 19:200
2. Gawalt ES, Avaltroni MJ, Koch N, Schwartz J (2001) Langmuir 17:5736
3. Hansson HA, Albrektsson T, Branemark PI (1983) J Prosthet Dent 50:108
4. Albrektsson T, Jacobsson M (1987) J Prosthet Dent 57:597
5. Tryoen TP, Vautier D, Haikel Y, Voegel JC, Schaaf P (2002) J Biomed Mater Res 60:657
6. Richert L, Lavalle P, Payan E, Shu XZ, Prestwich GD (2004) Langmuir 20:448
7. Omelon SJ, Grynpas MD (2008) Chem Rev 108:4697
8. Chen YX, Liu WM, Ye CF, Yu LG, Qi SK (2001) Mater Res Bull 36:2605
9. Paszternák A, Stichleutner S, Felhősi I (2007) Electrochim Acta 53:337
10. Schuler M, Tosatti S, Gruner P, Garg R, Textor M (2003) Stability of self-assembled alkane phosphate/phosphonate monolayers on smooth titanium oxide. Swiss Federal Institute of Technology, Switzerland, p 1

11. Hanson EL, Schwartz J (2003) JACS 16074
12. Danahy MP, Avaltroni MJ, Midwood KS, Schwarzbauer JE, Schwartz J (2004) Langmuir 20:5333
13. Silverman BM, Wieghaus KA (2005) Langmuir 21:225
14. Zhang YY, Hu R, Chen F, Lin CJ (2005) J Biomed Eng 22:618
15. Chen F, Yu Y, Li SB, Lian GB (2006) China Surfactant Deterg Cosmet 36:331
16. Fan HH, Chen YP, Qiu F (2007) Fine Chem 24:961
17. Beck JS (1992) J Am Chem Soc 114:10834
18. Duan R, Zhang JJ, Du XQ, Yao XC, Konno K (2009) Food Chem 112:702
19. Gurpreet SB, Graeme KH, Harvey AG (2008) Matrix Biol 27:600
20. Jonasova L, Muller FA, Helebran A, Strnad J, Greil P (2004) Biomaterials 25:1187
21. Uchida M, Kim HM, Kokubo T, Fujibayashi S, Nakamura T (2003) J Biomed Mater Res 64:164
22. Frateur I, Lecoeur J, Zanna S, Olsson COA, Landolt D, Marcus P (2007) Electrochim acta 52:7660
23. Diana T, Hughes W, Graham E (1996) Biomaterials 17:859
24. Diana T, Hughes W, Rachel CH, Graham E (1995) Biomaterials 16:697
25. Tang K, Yan J (2007) China Surfactant Deterg Cosmet 37:410
26. Liu Q, Ding J, Mante FK, Wunder SL, Baran GR (2002) Biomaterials 23:3103
27. Pimanpang S, Wang PI, Senkevich JJ, Wang GC, Lu TM (2006) Colloid Surf A 278:53
28. Chang MC, Tanaka J (2002) Biomaterials 23:4811
29. Liu GB, Guo L, Feng Q, Liu YJ, Wang WL, Liao KJ (2002) Optoelectron Technol 22:144
30. Wei JH, Feng XH, Zhang JR (2008) Chin J Conserv Dent 18:396
31. Wassell DTH, Hall RC, Embery G (1995) Biomaterials 16:697
32. Dewez JL, Berger V, Schneider YJ, Rouxhet PG (1997) J Colloid Interf Sci 191:1
33. Michiardi A, Aparicio C, Ratner BD, Planell JA, Gil J (2007) Biomaterials 28:586
34. Janocha B, Hegemann D, Oehr C, Brunner H, Rupp F, Gerstorfer JG (2001) Surf Coat Technol 142–114:1051
35. Eustathopolos N, Nicholas MG, Drevet B (1999) Wettability at high temperatures. Pergamon Press, Oxford
36. Weeraphat PO, Siwaporn M, Tang IM (2008) Mater Chem Phys 112:453
37. Rogers KD, Etok SE (2004) J Mater Sci 39:5747. doi: 10.1023/B:JMSC.0000040085.43633.8a
38. Zhang HY (2002) Biochemical tutorial. Sichuan University Press, Chengdu
39. Luong LH, Hong SI, Patel RJ, Outslay ME, Kohn DH (2006) Biomaterials 27:1175
40. Masami T, Takehisa M (1997) J Biomed Mater Res 34:305